ISSN 2303-4521

**PERIODICALS OF ENGINEERING AND NATURAL SCIENCES**
**Vol. 4 No. 2 (2016)**
**Available online at: http://pen.ius.edu.ba**

# Modeling of Distributed Generators in 13 Nodes IEEE Test Feeder

Henry Giovanni Pinilla
**Universidad Central**
**Bogotá, Colombia**
**hgpinillar@ucentral.edu.co**

Andrés Julián Aristizábal
**Universidad de Bogota Jorge Tadeo Lozano**
**Bogotá, Colombia**
**andresj.aristizabalc@utadeo.edu.co**

Carlos Andrés Forero
**Universidad de Bogota Jorge Tadeo Lozano**
**Bogotá, Colombia**
**carlosa.foreron@utadeo.edu.co**

***Abstract***
*This work aims to develop a model capable of evaluating the behavior of distributed energy resources in 13-nodes IEEE systems as a result of the change in the disconnector's opening protocol that creates a power generation island. The first scenario simulated a failure in the 632-671 line isolating the subsystem into two 375 kVA distributed generation units (DG) in the nodes 675 and 652. Likewise, a second scenario considered the aperture of the disconnector located between nodes 671 and 692 representing a 375 kVA DG feeding a 900 kVA load. The last scenario produced a three-phase failure modeling two 500 kVA DG units in the nodes 634 and 646 supplying an 800 kVA load.*

**Keywords:** Distributed Sources, Electric Simulation, Generation Model, Islanding Operation, Power Systems.

## 1. Introduction

The distributed generation is defined as the utilization of electric power external sources directly connected to an existing power distribution infrastructure. These sources are denoted as Distributed Generation (DG) [1]
The distributed generation is based on the production of electricity located near the demanding load and frequently installed in the same building. It considers a wide variety of technologies depending on the availability. Sometimes, this distribution is named "disruptive" due to its propensity to affect the electric networks in industries. Mostly, microturbines and fuel cells will be the dominant components of distributed generation systems that will affect the dynamic grid components. [2]
Recently, there are two main pullers of distributed generation systems. The first puller is the increasing interest in the utilization of sustainable and clean energy resources. Likewise, the second puller is the new direction of the policies defined by some governments which allow independent companies to sell electricity using existing transmission and distribution grids. [3] Therefore, small-scale generation industries could find new opportunities to participate in the local energy market.
Large-scale installations guarantee the regional supply; therefore, they are not considered as a DG unit. These units are independent small-scale systems connected to the infrastructure due to economic and logistics reasons. [2,4].
The people is having a raising interest in installing power plants capable of supplying their own demand and feeding the exceeds to the grid generating extra income. Consequently, governments could decrease the high investments in the power generation sector resulting in a lower energy price and a high-quality supply [5].
The classical application of symmetrical components to short circuit computation is based on the premise that the normal pre-fault network is symmetricaland with balanced loads; while this assumption is acceptableat the transmission level, it does not hold in many distribution system feeders where the number of phases is less thanthree [6].
Distribution networkanalysis can be carried out either using phase coordinates orsymmetrical components, with the choice mainly dependingon whether calculations in one domain lead to computationalperformance improvements[7].
Existen en la literatura diferentes estudios relacionados con el modelado de sistemas de distribución teniendo en cuenta diferentes métodos, configuraciones y elementos que han contribuido de manera significativa a la investigación de redes de distribución de energía eléctrica a nivel mundial [8 - 12].
This work aims to develop a model capable of evaluating the behavior of distributed energy resources in 13-nodes IEEE systems as a result of the change in the disconnector's opening protocol that creates a power generation island. The stability analysis exposed here allows identifying the performance of a radial distribution power system with different disturbances. Results are relevant in the planning and operation stages of a distributed generation system.



DOI: 10.21533/pen.v4i2.55

## 2. Material and methods

Typically, the structure of a distribution system is based on radial or tree like feeders, probably with loops, which are often operated as open rings. In these networks, measurements are mainly located at the feeder-heads, either as voltage measurements, active and reactive power measurements or as current measurements [13].

Unlike transmission and subtransmission systems, where real-time telemetry provides sufficient redundancy to assurenetwork observability, medium voltage (MV) distribution feedershave so far lacked the required infrastructure (sensorsand telecommunication) allowing the operating point to beaccurately determined [14].

Tests were performed using synchronous and asynchronous machines. The synchronous machines were based on smooth rotor units of 1.25 MVA capacity [15, 16]. These units were characterized using the software NEPLAN [17]. The transitory and sub transitory impedance sequences were needed in the short-circuit modeling. The parameters were defined in accordance to [18] and are summarized in table 1 and table 2.

Modeling the central generation unit was done using parameters gathered in Table 3. The simulations were performed using a 13-nodes IEEE radial system [19].

A 615 MVA synchronous generator capable of supplying the load was employed. This generator replaced the grid feeder used in the IEEE test model. It was necessary to add a 5 MVA power transformer which decreases the voltage from 15 kV at the generator outlet to 4.16 kV; this is the voltage set in the system [15, 16] (Figure 1).

*Table 1. Parameters Considered in the Synchronous Distributed Generation [18]*

| | | | |
|---|---|---|---|
| 0.4 – 1.25 MVA 0.48 kV | T'do = 5,51s | D = 0 | X''d = ,0171 |
| | T''do = 0,10s | Xd = 2,062 | X''q = 0,171 |
| | T'qo = 0,8s | Xq = 1,35 | Xl = 0,1 |
| | T''qo = 0,1s | X'd = 0,251 | S(1,0) = 0,176 |
| | H = 1,29s | X'q = 0,631 | S(1,2) = 0,49 |

*Table 2. Parameters of the Synchronous Distributed Generation Exciters [18].*

| | | |
|---|---|---|
| TR = 0,02s | VRMIN = -7,3 | TF = 1,0 |
| KA = 400 | KE = 1 | E1 = 5,475 |
| TA = 0,02s | TE = 0,253s | SE(E1) = 0,5 |
| VRMAX = 7,3 | KF = 0,03 | E2 = 7,3 SE(E1) = 0,86 |

*Table 3. Parameters considered in the central generation system [18]*

| | | | |
|---|---|---|---|
| 615MVA 15kV | T'do = 3,3s | D = 2 | X''d = 0,23 |
| | T''do = 0,02s | Xd = 0,898 | X''q = 0,2847 |
| | T'qo = 0,001s | Xq = 0,646 | Xl = 0,2396 |
| | T''qo = 0,06s | X'd = 0,2995 | S(1,0) = 0,18 |
| | H = 5,145s | X'q = 0,646 | S(1,2) = 0,33 |

The aerial distribution lines were set up according to the characteristic of impedance and distance between the phase conductors [20]. The dimensions of each line varied for each segment depending on the nodes location.

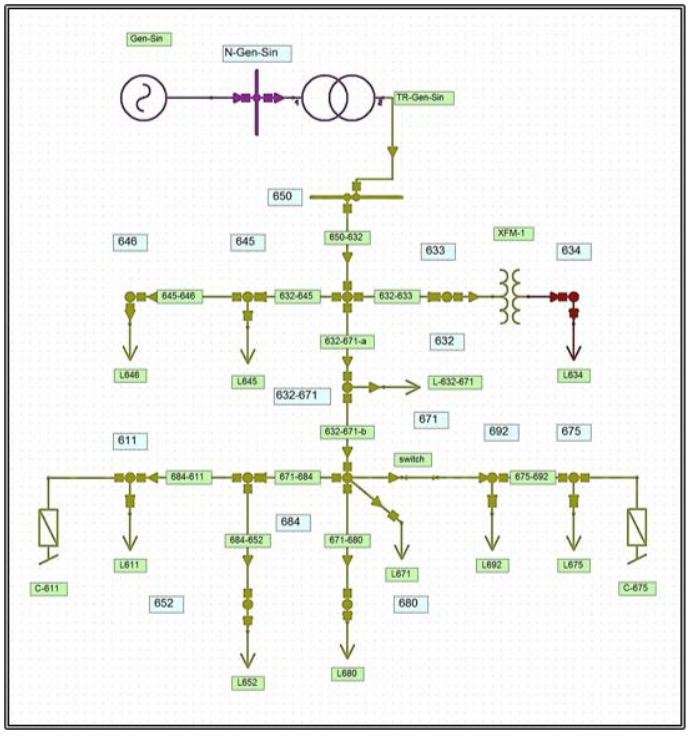


*Figure 1. Layout of the 13-nodes IEEE radial test system [19]*

Table 4 summarizes the impedance values and other configuration parameters.



DOI: 10.21533/pen.v4i2.55

*Table 4. Setup of the lines used in the 13-nodes IEEE radial test system [20]*

| Setup | R (ohm/mile) | X (ohm/mile) | B (μS/mile) | Ir max (A) |
|---|---|---|---|---|
| 601 | 0,3465 | 1,0179 | 6,2928 | 730 |
| 602 | 0,7526 | 1,1814 | 5,6990 | 340 |
| 603 | 1,3294 | 1,3471 | 4,7097 | 230 |
| 604 | 1,3228 | 1,3569 | 4,6658 | 230 |
| 605 | 1,3292 | 1,3475 | 4,5193 | 230 |
| 606 (sub) | 0,7982 | 0,4463 | 96,8897 | 329 |
| 607 (sub) | 1,3425 | 0,5154 | 88,9912 | 310 |

The excitation system of the synchronous machine was modeled using NEPLAN; a control block was fitted and the recommendations mentioned in [21] were followed as shown in Figure 2.

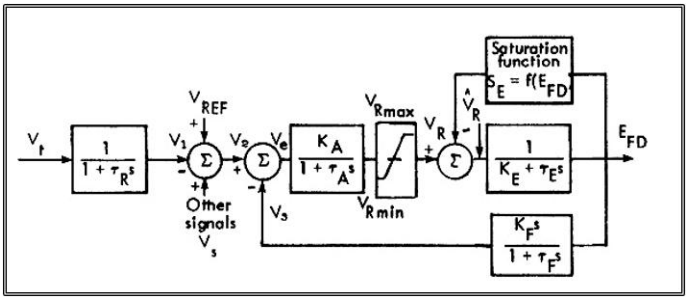


*Figure 2. Type 1 excitation system [22]*

The regulator of the excitation system works continuously in the model [22]. The control block and the synchronous generator were fitted, modeling the distributed generation system as shown in Figure 3.

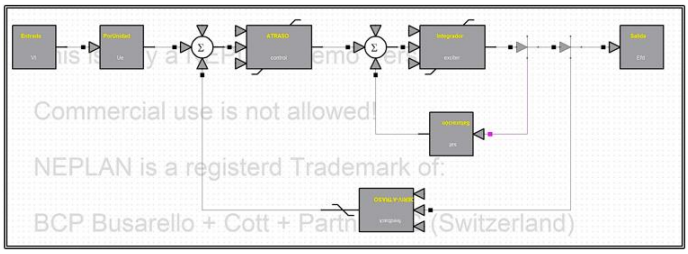


*Figure 3. Control block applied to the type 1 exciter*

The variables that were adjusted were included in Table 5. Parameters were defined in NEPLAN and the transference function was established [16].

Connecting the generators to the distribution grid was possible by using two transformer models. One is a 16 kV 15/4 reducer type that connects the central generation unit; whereas the second is a 16 kV 0.48/4 elevator type transformer which connects the synchronous generators to the nodes of the grid.

*Table 5. Configuration of the Exciter[20]*

| Symbol | Description | Value |
|---|---|---|
| TR | Time constant of the regulator input | 0.02 s |
| KA | Regulator gains | 400 |
| TA | Time constant of the regulator amplifier | 0.02 s |
| KE | Gain exciter | 1 |
| TE | Time constant exciter | 0.253 s |
| KF | Loop gain stabilization of the output voltage of the amplifier | 0.03 |
| TF | Time constant of the stabilization block | 1.0 s |
| VRMAX | Maximum regulator output voltage | 7.3 V |
| VRMIN | Minimum regulator output voltage | -7.3 V |
| E1 | Saturation Voltage | 5.475 V |
| SE75max | Exciter saturation function at 75 % | 0.5 |
| E2 | Saturation Voltage | 7.3 V |
| SEMAX | Exciter saturation function at 100 % | 0.86 |

Parameters were included in Table 6.

*Table 6. Transformers Configuration [20]*

| | S (KVA) | VH (kV) | VL (kV) | R % | X % |
|---|---|---|---|---|---|
| TR Gen-Sin | 5000 | 15 – D | 4,16 – Y | 1 | 8 |
| TR GD | 400 | 0,48 – D | 4,16 – Y | 1,1 | 5 |
| XFM-1 | 500 | 4,16 – Gr W | 0,48 – Gr W | 1,1 | 2 |

## 3. Results and discussion

### 3.1. Load flow analysis

The analysis of the steady state was done utilizing a load flow and the application of the Newton-Raphson method on the 13-node model. Based on this, we determined which nodes showed the largest drop on its voltage profile as shown in Table 7.

These are the most sensible nodes; therefore, they were considered as fundamental criteria to include the synchronous and asynchronous GD units together with the static and dynamic analysis [16]

The simulation of the system considering the central generation unit exclusively (Figure 1) exhibits that nodes 646 and 680 have the largest decrease in the voltage profile with values about 94.09 and 93.91%, respectively. These results are under the operational limit between 90 and 110%.


DOI: 10.21533/pen.v4i2.55

Table 7. Results of the Load Flow of the 13-node IEEE System.

| MS 13 N | | | | | | | | |
|---|---|---|---|---|---|---|---|---|
| Node | U kV | U % | Node | U kV | U % | Node | U kV | U % |
| 646 | 3,91 | 94,09 | 684 | 3,938 | 94,6 | 675 | 3,928 | 94,42 |
| 645 | 3,92 | 94,26 | 611 | 3,934 | 94,5 | N-Gen-Sin | 16,5 | 110 |
| 633 | 4,11 | 98,99 | 652 | 3,929 | 94,4 | 650 | 4,421 | 106,29 |
| 671 | 3,94 | 94,83 | 680 | 3,903 | 93,8 | N 632-671 | 4,034 | 96,97 |
| 634 | 0,45 | 95,03 | 692 | 3,943 | 94,7 | 632 | 4,134 | 99,37 |

### 3.2. Voltage stability

The voltage stability was studied doing several simulations of continuous load flow; these were performed varying the operational control of the DG unit in the PV or PQ mode, and changing the load factor when the asynchronous DG unit was added.

Figures 4 and 5 exhibit the effects that these changes have on the voltage stability observable in the voltage profile of the node 632. Results provide insights about the voltage collapse when the power transferences increases in a specific region of the radial system; nonetheless, the collapse point for all the nodes occurs at the same power level regardless of the voltage observable in the specific nodes.

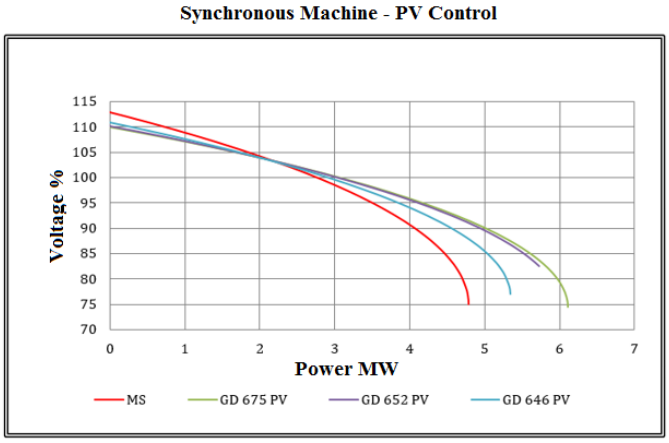


*Figure 4. PV control on node 632*

As a result of installing a generation unit in the node 675, 653 and 646, the stability of the systems and the load factor "λ" will rise in comparison to the base case where the load flow was done using the central generation unit solely (Figure 4). After adding the DG unit at the node 675, the chargeability moves up to 6.076 MW with a voltage collapse level of 77.305 V% .

Figure 5 shows the performance of the system when controlling the operation of the PQ machine.

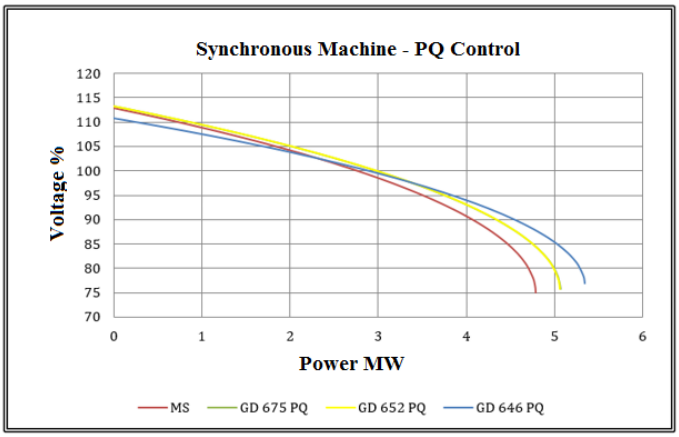


*Figure 5. PQ control on node 632*

The load factor in the node 646 and the voltage collapse level augmented up to 0.545 MW and 78.419 V% in comparison with the MS. This means that the load factor does not depend on the time; likewise, as a result of the change in this factor, the equilibrium points, and the system trajectories vary.

Simulations of the asynchronous machine (figure 6) exhibit that the load factor of the DG unit is lower than the 4.772 MW resulting from the central distribution system.

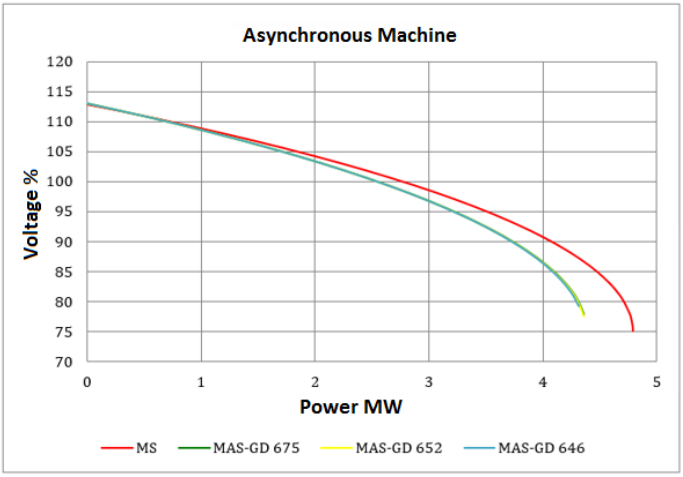


*Figure 6. Asynchronous machine, node 632*

Meanwhile, the voltage collapse limit is 77.093V% which reduces the stability margin of the system. This can be ascribed to the fact that asynchronous machines are not capable of generating reactive power.

It is noted that the profiles voltage increases in the most critical nodes.This indicates that the stability for the load increases when machines of generation are installed close or where larger loads are.Voltage profiles at 680 and 646 nodes increased approximately 3%.It is also noted that the voltage profile varies around 1.5% and depending on the


DOI: 10.21533/pen.v4i2.55

point of location on the network; profile increases by approximately 2%.This is very positive because if a disturbance occurs in the system, it is capable of returning in an acceptable time to a steady state where the voltages in all nodes are within an operating range.

### 3.3. Islanding operation analysis

Islanding operation conditions were adjusted by adding generation units in the nodes 675 – 652 – 646 – 634.

Afterward, three scenarios were simulated to analyze possible real failures in grids with distributed generation.

#### 3.3.1. Failure in a line

The first scenario assumed a failure in the line 632-671 isolating the subsystem into two 375 kVA DG units in the nodes 675 and 652. These units fed a 1.7 MVA load as exhibited in figure 7.

A three-phase failure was promoted in the line in two seconds, and then an answer was observed in the switch located at node 671 which solve the failure in three seconds.

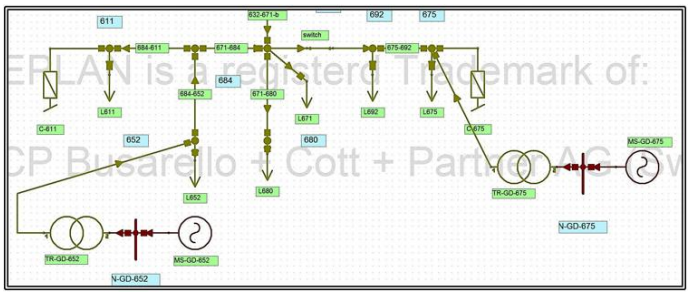


*Figure 7. Layout of the system under islanding operation*

Figure 8 shows the effect of the failure on the line. There is an oscillation that is supported by the central generation unit together with the two DG units and their corresponding excitation systems; nevertheless, the frequency gets out of synchrony when the switch placed at node 671 is opened.

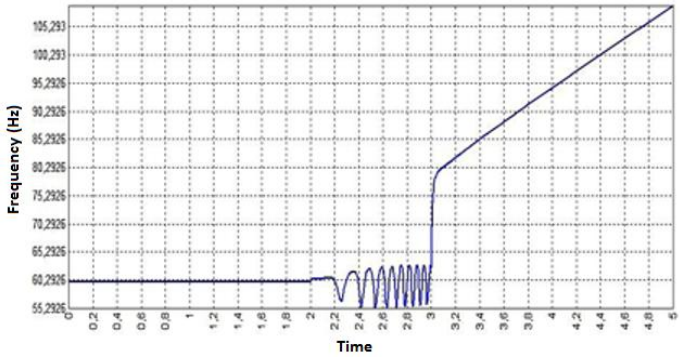


*Figure 8. Performance of the frequency*

Meanwhile, the DG units raise their frequency out of control because the central generation unit was supported the operational frequency of the radial network initially.

The active power provided by each unit undergoes some changes due to the failure simulated (Figure 9).

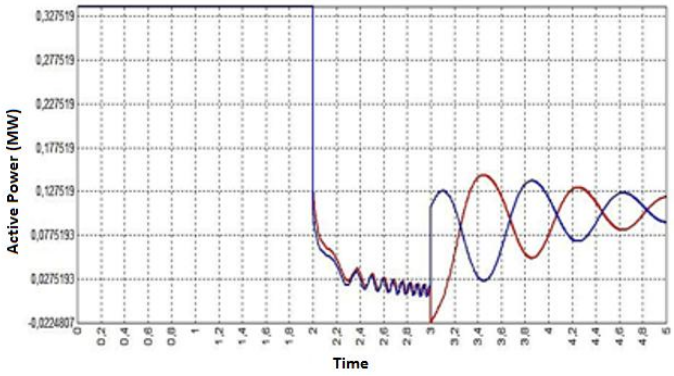


*Figure 9. Performance of the active power*

Exactly 2s of the simulation,active power experiences a fall from 0,33MW until 0,077MW; point which has a reaction to 3s and then unexpectedly increases to a peak value of 0,13MW. These results of active power, can be used to resize correctly, electrical networks that work with distributed generation; as the active power flow in both directions, grid becomes dynamic and this affects the size of the conductorsand protection systems.

As a consequence of this disruption, there is a tension collapse as shown in the node 671 (Figure 10).

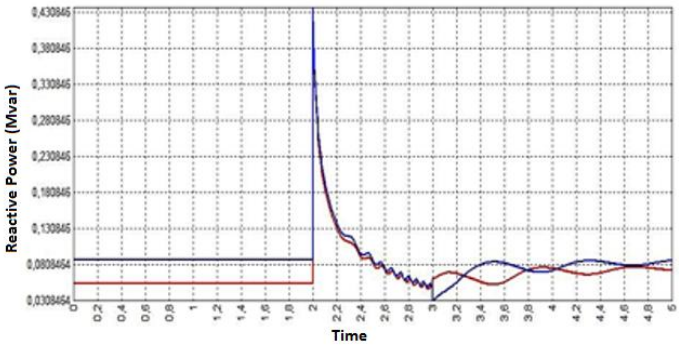


*Figure 10. Results of the reactive power in the node 671*

Furthermore, there is a less sensitive response when the DG units are asynchronous machines. Figure 11 exhibits the frequency oscillation when the failure occurs.

This parameter is recovered increasing the stability of the DG units after disconnecting the line 671.



DOI: 10.21533/pen.v4i2.55

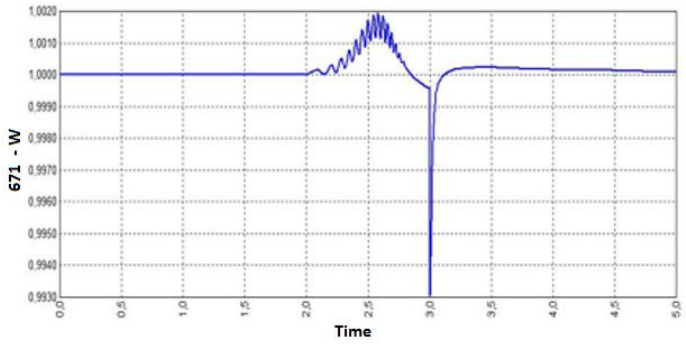


*Figure 11. Frequency oscillation registered*

These simulations show that the use of distributed generation sources increases the oscillation frequency of the 13 nodes system and these frequency oscillations are larger when asynchronous machines around 5.09 Hz are used.

Nonetheless, the active power drops to zero consequently with the voltage collapse as shown in Figure 12.

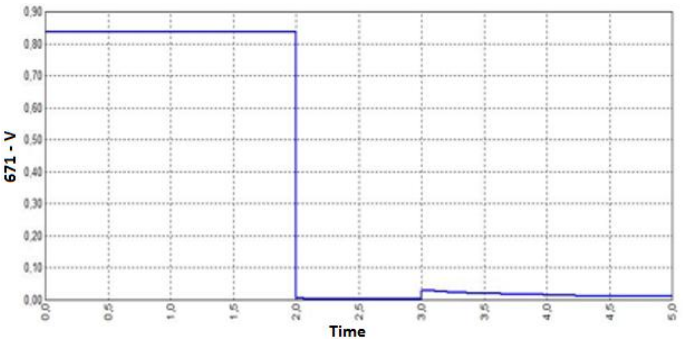


*Figure 12. Voltage collapse registered in the node 671*

This is ascribed to the high load demanded by the system in comparison with the power produced by the DG units. Finally, the reactive power, which DG units cannot supply, is satisfied by the shunt capacitance connected to nodes 611 and 675 (Figure 13).

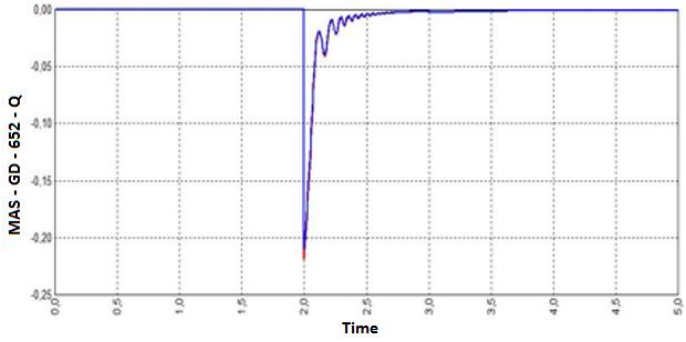


*Figure 13. Effect of the shunt capacitance connected to nodes 611 and 675*

### 3.3.2. Open a disconnector

The second scenario is simulated by opening the disconnector located between node 671 and 692. As a result of it, there is a 375 kVA DG unit feeding a 900 kVA load (Figure 14).

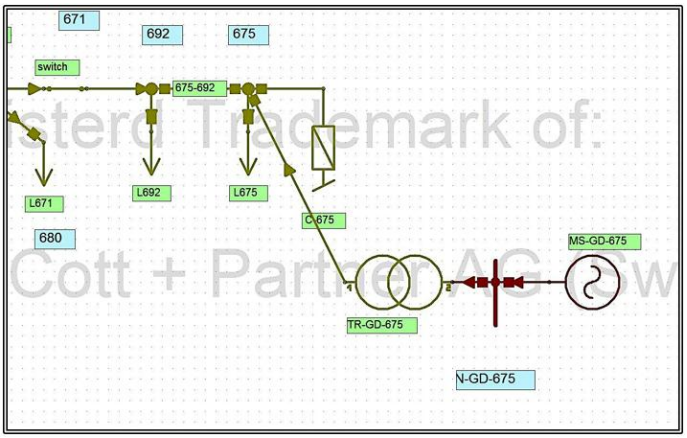


*Figure 14. Layout of the system under conditions described in the scenario II*

Disconnector is opened at 2s. Similarly as the scenario mentioned above, the disconnector aperture affects the synchrony of the system as shown in Figure 15.

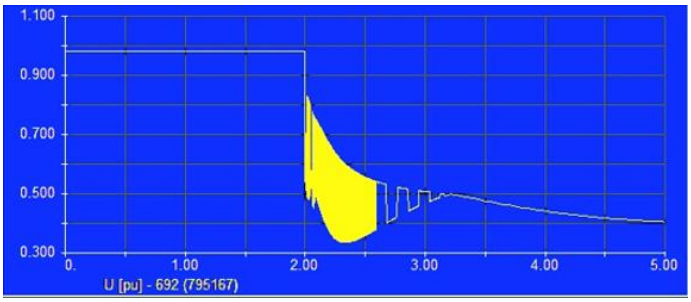


*Figure 15. Voltage at node 692*

The differences between the demand and the power capacity of the DG units produce a voltage collapse.

### 3.3.3. A three-phase failure

The third scenario consists of a three-phase failure occurring in the line 632 – 671 at 2s. The impedance and distance relays located in node 632 sense the failure, opening the disconnector attached to line 761 0.1 s later. Afterward, the impedance relay disconnects the central generation unit. This scenario models a system composed of two DG units in the nodes 634 and 646 with a power capacity of 500 kVA each one capable of supplying an 800 kVA load as stated in Figure 16.



DOI: 10.21533/pen.v4i2.55

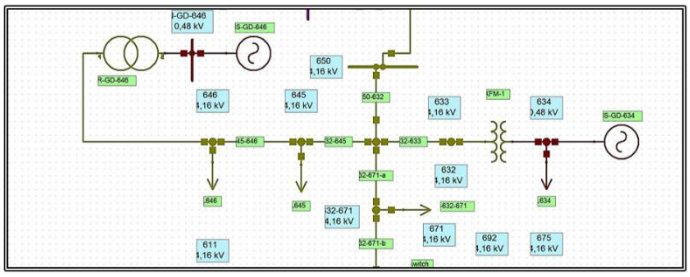

*Figure 16. Layout of the system under conditions described in the scenario III*

The performance of the two DG units is summarized in Figure 17.

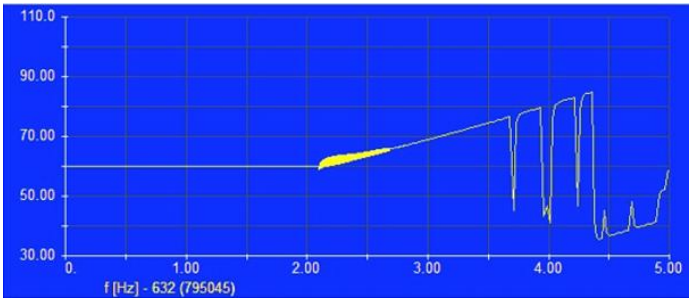


*Figure 17. Frequency at node 632*

The system frequency stabilizes after disconnecting the central generation unit; although, three seconds later, it varies again due to the load supplied by the two DG units. This load causes instability in the DG units, and a voltage collapse caused by the active power (Figure 18).

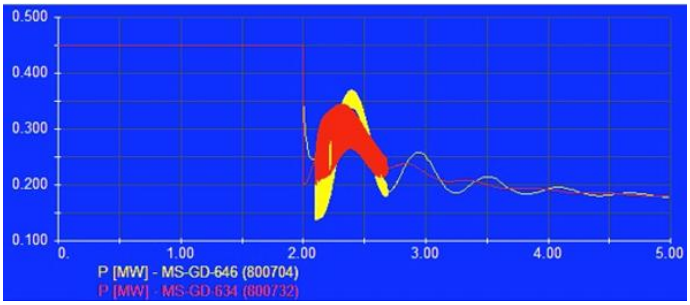


*Figure 18. Active power in the GD units*

## 4. Conclusions

The behavior of distributed energy resources in 13-nodes IEEE systems as a result of the change in the disconnectors´ opening protocol that creates a power generation island was modeled. The islanding operation of a power network consisting of distributed generation units have some security and stability problems that need to be considered. To keep the system operating conditions should be used controls and protections that detect failures and minimize their duration in the system, as recommended by the IEEE P1547.4 standard is a guide to the design, operation and integration of distributed generation systems in islanding power systems.

In cases where the system instability occurs and the island load is higher than the DG units capacity, protection measurements should be considered to sense the dynamic performance of the system and adjust the DG units or disconnect them when needed. Hence, voltage profile collapses can be avoided. Distance and impedance relays should be correctly parametrized because this can promote instabilities that will affect the dynamic response, cause large oscillations, and modify the power angle of the Dg units.

The adequate operation of the systems analyzed with DG units depends on the DG power capacity; it might be larger than the electrical load. The power balance should be preserved considering the synchronous or asynchronous characteristics of the machines. Also, AVR and PSS devices fitted to the generation units should be employed allowing to stabilize the system against fast and slow disturbances such as an aperture of switches, disconnectors, reconnectors, or changes in the load profile.


## Acknowledgements

Authors kindly acknowledge the financial support of the Universidad de Bogotá Jorge Tadeo Lozano under the project code 633-11-14.


## 5. References


[1] J. E. Kim, H. K. Tetsuo and Y. Nishikawa, "Methods of determining introduction limits of Dispersed Generation systems in a distribution system", ScriptaTechnica, Kyoto University, Japan, 1997.

[2] F. Jurado, J. Carpio. "Enhancing the distribution networks stability using distributed generation". The International Journal for Computation and Mathematics in Electrical and Electronic Engineering, Vol. 24, No 1, 2005.

[3] C. P. Lawrence, M. M. A. Salama and R. El Shatshat. "Studying the effects of distributed generation on voltage regulation", International Journal of Electrical Engineer Education, Vol. 46, issue 1, 2008.

[4] R. C. Dugan and T. E. McDermott, "Operating conflicts for distributed generation on distribution systems", in Proc. IEEE Rural Electric Power Conference 2001, pp. A3/1–A3/6.

[5] N. Mithulananthanand Than O. "Distributed generatos placement to maximize the loadability of a distribution system", International Journal of Electrical Engineer Education, Vol. 43, issue 2, 2006.

[6] R. A. Jabr and I. Dzafic, "A Fortescue Approach for Real-Time Short Circuit Computation in Multiphase Distribution Networks," IEEE Trans. Power Syst., vol. 30, no. 6, pp. 3276–3285, Nov 2015.

[7] I. Dzafic, R. A. Jabr, and H. T. Neisius, "Transformer modeling for three-phase distribution network analysis," IEEE Trans. Power Syst., vol. 30, no. 5, pp. 2604–2611, Sept 2015.






DOI: 10.21533/pen.v4i2.55

[8] I. Dzafic, R. A. Jabr, E. Halilovic, and B. C. Pal, "A sensitivity approach to model local voltage controllers in distribution networks," IEEE Trans. Power Syst., vol. 29, no. 3, pp. 1419–1428, May 2014.
[9] I. Dzafic, B. C. Pal, M. Gilles, and S. Henselmeyer, "Generalized PI Fortescue equivalent admittance matrix approach to power flow solution," IEEE Trans. Power Syst., vol. 29, no. 1, pp. 193–202, Jan. 2014.
[10] I. Dzafic, M. Gilles, R. A. Jabr, B. C. Pal, and S. Henselmeyer, "Real time estimation of loads in radial and unsymmetrical three-phase distribution networks," IEEE Trans. Power Syst., vol. 28, no. 4, pp. 4839–4848, Nov. 2013.
[11] I. Dzafic, H. T. Neisius, M. Gilles, S. Henselmeyer, and V. Landerberger, "Three-phase power flow in distribution networks using Fortescue transformation," IEEE Trans. Power Syst., vol. 28, no. 2, pp. 1027–1034, May 2013.
[12]A. Gomez-Exposito, E. Romero-Ramos, and I. Dzafic, "Hybrid real–complex current injection-based load flow formulation", Electric Power Systems Research, vol. 119, pp. 237-246, Feb. 2015.
[13] I. Dzafic, I. Huseinagic, and S. Henselmeyer, "Real time distribution system state estimation based on interior point method," Southeast Europe Journal of Soft Computing, vol. 3, no. 1, pp. 32–38, Mar. 2014.
[14] A. Gomez-Exposito, C. Gomez-Quiles, and I. Dzafic, "State estimation in two time scales for smart distribution systems," IEEE Trans. Smart Grid, vol. 6, no. 1, pp. 421–430, Jan. 2015.
[15] Distribución Eléctrica Inteligente SILICE – Fase II, CODENSA, Universidad Nacional de Colombia, Universidad de los Andes, Colciencias, Septiembre de 2010.
[16] H. Pinilla, A.J. Aristizábal. "Análisis en estable y transitorio de fuentes de generación distribuida operando en isla", Revista Elementos, Numero 5, 2015.
[17] Software Neplan. [En línea]. Disponible: http://www.neplan.ch/neplanproduct/en-electricity/
[18] Abdel-Aziz A. Fouad Paul M. Anderson. Power System Control and Stability. IEEE Press, 2003.
[19] W. H. Kersting. Radial distribution test feeders. Technical report, IEEE Distribution System Analysis Subcommittee, 2000.
[20] IEEE Distribution Planning Working Group Report, "Radial distribution test feeders", IEEE Transactioins on Power Systems,, August 1991, Volume 6, Number 3, pp 975-985.
[21] IEEE Std 421.5-1992, IEEE Recommended Practice for Excitation System Models for Power System Stability Studies.
[22] Computer Representation of Excitation Systems, IEEE COMMITTEE REPORT, IEEE TRANSACTIONS ON POWER APPARATUS AND SYSTEMS, VOL. P.AS-87, No. 6 JUNE 1968.



DOI: 10.21533/pen.v4i2.55